ANNUAL REVIEWS

Annual Review of Nuclear and Particle Science

Mixing and *CP* Violation in the Charm System

Alexander Lenz[1] and Guy Wilkinson[2]

[1]Department Physik, Universität Siegen, 57068 Siegen, Germany;
email: Alexander.Lenz@uni-siegen.de

[2]Department of Physics, University of Oxford, Oxford OX1 3RH, United Kingdom;
email: Guy.Wilkinson@physics.ox.ac.uk

Annu. Rev. Nucl. Part. Sci. 2021. 71:59–85

First published as a Review in Advance on April 14, 2021

The *Annual Review of Nuclear and Particle Science* is online at nucl.annualreviews.org

https://doi.org/10.1146/annurev-nucl-102419-124613

Keywords

charm physics, neutral meson mixing, *CP* violation

Abstract

In recent years charm physics has undergone a renaissance, which has been catalyzed by an unexpected and impressive set of experimental results from the *B* factories, the Tevatron, and LHCb. The existence of $D^0\bar{D}^0$ oscillations is now well established, and the recent discovery of *CP* violation in D^0 decays has further renewed interest in the charm sector. In this article, we review the current status of charm-mixing and *CP*-violation measurements and assess their agreement with theoretical predictions within the Standard Model and beyond. We look forward to the great improvements in experimental precision that can be expected over the coming two decades and to the prospects for corresponding advances in theoretical understanding.

Contents

1. INTRODUCTION

Charm played a pivotal role in the construction of the Standard Model (SM). Its existence was invoked in the discovery of the GIM mechanism (1), and it was the observation of the J/ψ particle in 1974 that convinced the community of the validity of the quark model (2, 3). It was soon appreciated that mixing and *CP*-violating phenomena are expected to manifest themselves at a considerably lower level in charm than in the beauty system, and indeed for many years all searches for such effects were frustrated. The last 15 years, however, have seen enormous experimental progress, a trajectory that looks set to continue over the coming two decades.

In this review we summarize the experimental and theoretical status of charm-mixing and *CP*-violation studies. We describe the key measurements that have established our current understanding, and we look forward to the advances that can be expected in the coming years. We discuss the theoretical tools that have been developed to confront the data, and we pay particular attention to the challenges that charm studies bring in this respect. We stress the great potential of charm for revealing signs of physics beyond the SM (BSM) and assess some of the most interesting existing experimental results in this context.

2. THEORETICAL FRAMEWORK

In this review we consider $D^0\bar{D}^0$ mixing and direct *CP* violation in singly Cabibbo-suppressed (SCS) decays $c \to s\bar{s}u$ (e.g., $D^0 \to K^+K^-$) and $c \to d\bar{d}u$ (e.g., $D^0 \to \pi^+\pi^-$). SCS decays have a penguin contribution in addition to the tree-level contribution, leading to the possibility of *CP*-violating effects, unlike Cabibbo-favored (CF) decays $c \to s\bar{d}u$ (e.g., $D^0 \to \pi^+K^-$) and doubly Cabibbo-suppressed (DCS) decays $c \to d\bar{s}u$ (e.g., $D^0 \to K^+\pi^-$), which cannot have penguin contributions.

To sum up large logarithms of the form $\alpha_s(m_c)^m \ln^n(m_c^2/M_W^2)$ $(m \geq n)$ to all orders, weak decays of charmed hadrons are treated via the effective Hamiltonian $\mathcal{H}_{\text{eff}}$, where all heavy (i.e., heavier than the charm quark) degrees of freedom have been integrated out (for more details, see, e.g.,

Reference 4). Here,

$$\mathcal{H}_{\rm eff} = \frac{G_F}{\sqrt{2}} \left\{ \lambda_d \left[C_1(\mu) Q_1^d + C_2(\mu) Q_2^d \right] + \lambda_s \left[C_1(\mu) Q_1^s + C_2(\mu) Q_2^s \right] + \lambda_b \sum_{i \geq 3} C_i(\mu) Q_i \right\}, \qquad 1.$$

with the Cabibbo–Kobayashi–Maskawa (CKM) (5, 6) structures $\lambda_x = V_{cx} V_{ux}^*$. The Wilson coefficients $C_i(\mu)$ have been calculated in perturbation theory (see, e.g., Reference 7). Q_1 and Q_2 denote tree-level four-quark operators

$$4Q_1^q = \bar{q}^\alpha \gamma_\mu (1-\gamma_5) c^\beta \times \bar{u}^\beta \gamma^\mu (1-\gamma_5) q^\alpha, \; 4Q_2^q = \bar{q}^\alpha \gamma_\mu (1-\gamma_5) c^\alpha \times \bar{u}^\beta \gamma^\mu (1-\gamma_5) q^\beta, \qquad 2.$$

where α and β are color indices. $Q_{i \geq 3}$ denote penguin operators (i.e., those concerned with loop-induced $c \to u$ transitions), where the heavy b quark and the W boson have been integrated out. The unphysical renormalization scale dependence of the Wilson coefficients cancels order-by-order with the μ dependence of the matrix elements of the four-quark operators. Amplitudes describing the decay of a neutral D meson into a final state f are denoted by

$$A_f = \langle f | \mathcal{H}_{\rm eff} | D^0 \rangle; \; \bar{A}_f = \langle f | \mathcal{H}_{\rm eff} | \bar{D}^0 \rangle; \; A_{\bar{f}} = \langle \bar{f} | \mathcal{H}_{\rm eff} | D^0 \rangle; \; \bar{A}_{\bar{f}} = \langle \bar{f} | \mathcal{H}_{\rm eff} | \bar{D}^0 \rangle. \qquad 3.$$

Weak decays and mixing of hadrons containing a charm quark show several peculiarities compared with decays of b hadrons, which make their theoretical description considerably more challenging. First, the corresponding CKM elements are to a large extent real and therefore do not leave much space for *CP*-violating effects. According to the web update of Reference 8 (for similar results, see Reference 9), we find for the central values of the CKM elements involving the charm quark

$$V_{cd} = -0.2245 - 2.6 \times 10^{-5} i, \qquad V_{cs} = 0.97359 - 5.9 \times 10^{-6} i, \quad V_{cb} = 0.0416. \qquad 4.$$

These numbers were determined assuming the validity of the SM and in particular the unitarity of the CKM matrix, and they might change in the presence of BSM effects. Moreover, the value of a single matrix element is unphysical and depends on the phase convention, which was chosen here such that V_{cb} is real. In D mixing and SCS D meson decays, the physical combinations $\lambda_q = V_{cq} V_{uq}^*$ will arise. We find as central values

$$\lambda_d = -0.21874 - 2.51 \times 10^{-5} \, i, \qquad 5.$$

$$\lambda_s = +0.21890 - 0.13 \times 10^{-5} \, i, \qquad \lambda_b = -1.5 \times 10^{-4} + 2.64 \times 10^{-5} \, i. \qquad 6.$$

Again we observe for λ_d and λ_s only negligible imaginary parts, and their real parts are of almost exactly the same size but of opposite sign. Thus, the unitarity relation $\lambda_d + \lambda_s + \lambda_b = 0$ is fulfilled to a good approximation for the first two generations alone—that is, $\lambda_d + \lambda_s \approx 0$. This is one of the two reasons why the GIM mechanism (1) can be extremely pronounced in the charm sector. The modulus of λ_b is much smaller than that of $|\lambda_{d,s}|$, but its imaginary part has a similar size as its real one. Therefore, this latter CKM combination could be important for the potential size of *CP* violation in the charm system within the SM.

Next, we find that in loop contributions arising in D mixing or in penguin contributions, the charm quark can transform into an internal d, s, or b quark, as indicated in **Figure 1**. In the case of b hadron decays, the corresponding internal quarks would be u, c, and t. The loop functions

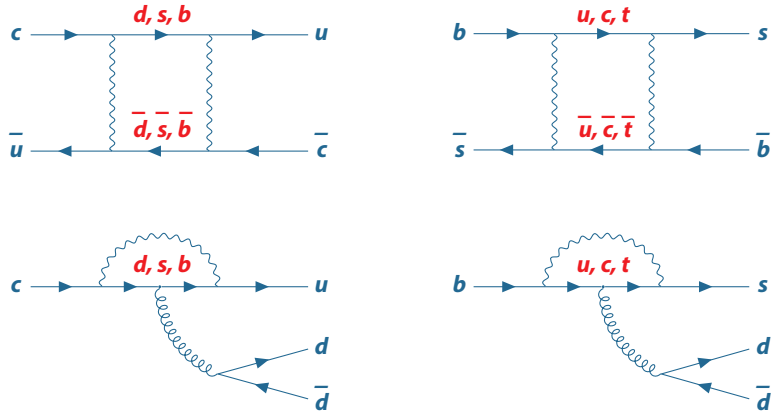

Figure 1

Internal quarks in loop-induced transitions (neutral meson mixing in *top line* and penguin decays in *lower line*) of D and B mesons.

depend on the square of the virtual quark mass divided by the W boson mass. We thus find the following size of loop-function parameters in the charm and the beauty sector:

$$\left(\frac{m_d}{M_W}\right)^2 \approx 0, \qquad \left(\frac{m_u}{M_W}\right)^2 \approx 0, \tag{7.}$$

$$\left(\frac{m_s}{M_W}\right)^2 \approx 1.3 \times 10^{-6}, \quad \left(\frac{m_c}{M_W}\right)^2 \approx 2.5 \times 10^{-4}, \tag{8.}$$

$$\left(\frac{m_b}{M_W}\right)^2 \approx 2.8 \times 10^{-3}, \quad \left(\frac{m_t}{M_W}\right)^2 \approx 4.5. \tag{9.}$$

Hence, in the charm sector all internal masses are very close to zero and therefore largely identical—for identical quark masses, the GIM mechanism gives a zero result. This is the second reason for the severeness of the GIM mechanism in the charm sector, in contrast to the b system, where the large value of the top quark mass strongly breaks the GIM mechanism.

A third peculiarity is that the value of the charm quark mass is close to the hadronic scale $\Lambda_{\rm QCD}$, which makes the applicability of a Taylor expansion in $\Lambda_{\rm QCD}/m_c$ a priori questionable. This uncertainty should, however, be resolved by an as-precise-as-possible determination of the expansion parameter $\langle Q \rangle/m_c$ with theoretical state-of-the-art methods and not by simple dimensional analysis. Observables that are not affected by severe GIM cancellations—for example, lifetimes of charmed hadrons—are much better suited than, for example, D mixing for studying this issue.

Finally, the value of the strong coupling at the charm scale, $\alpha_s(m_c)$, is large. At five-loop accuracy at the charm pole mass scale ($m_c = 1.67$ GeV), we have

$$\alpha_s(m_c) = 0.33 \pm 0.01. \tag{10.}$$

This large value clearly points toward the important effect of higher-order perturbative contributions and perhaps even to the existence of sizeable nonperturbative effects.

3. EXPERIMENTAL OVERVIEW

Almost all measurements on CP violation and mixing discussed in this review were performed either at BaBar and Belle, the e^+e^-B-factory experiments that operated in the first decade of the

Table 1 Reported and expected signal yields in example decay modes, flavor-tagged through the process $D^{*+} \to D^0\pi^+$, and including semileptonic tags for the LHCb yields in $D^0 \to K^0_S\pi^+\pi^-$

	$D^0 \to K^+\pi^-$		$D^0 \to \pi^+\pi^-\pi^0$		$D^0 \to K^0_S\pi^+\pi^-$	
BaBar/Belle	11.5K	1.0 ab^{-1} (10)	126K	0.5 ab^{-1} (11)	1.2M	0.9 ab^{-1} (12)
CDF	32.7K	9.6 fb^{-1} (13)	NM		0.3M	6.0 fb^{-1} (14)
LHCb	722K	5.0 fb^{-1} (15)	566K	2.0 fb^{-1} (16)	2.3M	3.0 fb^{-1} (17)
Belle II	225K	50 ab^{-1} (18)	13M	50 ab^{-1}	67M	50 ab^{-1} (18)
LHCb Upgrade I	25M	50 fb^{-1} (19)	44M	50 fb^{-1}	598M	50 fb^{-1} (19)
LHCb Upgrade II	170M	300 fb^{-1} (19)	291M	300 fb^{-1}	3,990M	300 fb^{-1} (19)

The $D^0 \to \pi^+\pi^-\pi^0$ expectations are scaled from the existing measurements according to the ratio of integrated luminosities and, for the LHCb upgrades, accounting for a change in cross section with collision energy. A factor two improvement in trigger efficiency is also assumed for LHCb Upgrades I and II. Abbreviation: NM, not measured.

millennium, or at CDF and LHCb, hadron collider experiments situated at the Tevatron and the LHC, respectively. **Table 1** shows the signal yields at these experiments for three example decay modes.

At the *B* factories, charm hadrons are studied through their continuum production. The process $e^+e^- \to \gamma^* \to c\bar{c}$ has a cross section of around 1.3 nb at $\sqrt{s} = 10.58$ GeV, which exceeds that of $e^+e^- \to \Upsilon(4S)$. The low-multiplicity environment allows the efficient reconstruction of many decay modes, including those that involve π^0 mesons. In measurements that require knowledge of the initial flavor of the neutral charm meson of interest, this information is obtained by flavor-tagging this meson through the strong decay $D^{*+} \to D^0\pi^+$. Here the accompanying particle is named the slow pion because of its low momentum in the D^{*+} rest frame. Its charge distinguishes between D^0 and $\bar{D}^0$ mesons.

At hadron machines, the most prolific source of charm is through prompt production in the initial pp (or $p\bar{p}$) collision. Here the cross section is enormous; for example, $\sigma(pp \to c\bar{c}X) = (2{,}369 \pm 192)$ μb at $\sqrt{s} = 13$ TeV within the approximate acceptance of LHCb (20). The main challenge in exploiting these events lies in the triggering, as most of the decays of interest are fully hadronic, and the decay products have relatively low transverse momentum. Only experiments with dedicated heavy-flavor triggers, such as LHCb and CDF, have been successful in accumulating large samples through this source. As at the *B* factories, neutral mesons may be flavor-tagged through D^{*+} decays.

Analyses have also been performed at LHCb that make use of secondary production, where the charmed particle arises from the semileptonic decay of a *b* hadron. Although the cross section for beauty production is around 20 times lower than that of charm, the events are relatively easy to select because of the high efficiency for triggering semileptonic *b* hadron decays. The charge of the muon also provides a flavor tag. A final benefit of such a sample is that the selection efficiency is relatively uniform with decay time, in contrast to a prompt sample in which the trigger requirements tend to reject decays with low lifetimes. It also should be noted that secondary-charm production (not necessarily in semileptonic decays) contaminates the prompt samples, typically at the percent level and growing with decay time. In time-dependent measurements this contamination induces a bias, as the birth coordinate of the secondary D^0 meson is wrongly assigned to the primary vertex associated with the pp collision.

Studies performed at e^+e^- machines at and just above charm threshold make an important contribution to our knowledge of charm physics. The CLEO-c experiment collected 0.8 fb^{-1} of data at the $\psi(3770)$ resonance, and BESIII has so far accumulated 2.9 fb^{-1}, with the expectation of increasing this total to around 20 fb^{-1} (21). Although the sample sizes are not large enough to permit competitive *CP*-violation and mixing studies, the very clean environment and lack of

fragmentation particles permit unique measurements of branching ratios, *CP*-conserving strong phases, and associated parameters, which are important inputs to analyses performed at other facilities. Many of the results are achieved through a double-tag technique in which both charm mesons are reconstructed and measurements can benefit from the quantum coherence of the final state (e.g., see Reference 22).

Over the coming decade, results of ever-increasing sensitivity are expected from LHCb, which is currently undergoing an upgrade (Upgrade I) that will allow for operation at higher luminosity. The goal is to increase the integrated luminosity of the experiment from the 3 fb^{-1} (Run 1 at 7 TeV and 8 TeV) plus 6 fb^{-1} (Run 2 at 13 TeV) currently on tape to a total of 50 fb^{-1}. A full software trigger will be deployed that will significantly improve efficiency for many decays, particularly in charm physics. The LHCb results will be complemented by measurements from Belle II, which is now collecting data and aims to accumulate around 50 ab^{-1} of integrated luminosity (18). Plans are evolving for an Upgrade II of LHCb, which will operate in the next decade and allow the experiment to collect a total data set of 300 fb^{-1} (19). **Table 1** includes the predicted signal yields for these projects, which illustrate well the enormous increase in statistical precision that can be expected. If approved, a Super Tau Charm Factory will run in the 2030s in China and will have the potential of integrating $\mathcal{O}(1\ \text{ab}^{-1})$ at the $\psi(3770)$ resonance (23). A similar facility is proposed to be located in Novosibirsk, Russia (24).

Some other planned experiments that are of very different natures from those discussed above would also be suitable for performing precise studies in charm physics. The FCC-ee, scheduled to operate in the 2040s, would produce around 6×10^{11} $c\bar{c}$ pairs from Z^0 decays in a relatively clean analysis environment (25). CEPC in China would have similar capabilities. Another idea is to allow a high-intensity proton beam, such as that proposed for the Beam Dump Facility at CERN, to impinge on a system of tungsten targets, which would then produce charm hadrons in a quantity comparable to that at LHCb Upgrade II (see discussion of the TauFV experiment in References 26, 27).

4. THE $D^0\bar{D}^0$ SYSTEM: MIXING AND *CP* VIOLATION IN MIXING

4.1. Mixing Formalism for Neutral *D* Mesons

The weak eigenstates of the neutral D mesons [$D^0 = (c\bar{u})$ and $\bar{D}^0 = (\bar{c}u)$ with the convention $CP|D^0\rangle = -|\bar{D}^0\rangle$ and $CP|\bar{D}^0\rangle = -|D^0\rangle$, which is assumed throughout this review] mix under the weak interaction, and the time evolution of the neutral D mesons is governed by the mass eigenstates $D_{1,2} = pD^0 \mp q\bar{D}^0$. Diagonalization of the 2×2 matrix describing this mixing gives the following eigenvalue equations:

$$\Delta M_D^2 - \frac{\Delta\Gamma_D^2}{4} = 4\left|M_{12}^D\right|^2 - \left|\Gamma_{12}^D\right|^2 =: a,\ \Delta M_D \Delta\Gamma_D = 4\left|M_{12}^D\right|\left|\Gamma_{12}^D\right|\cos(\phi_{12}^D) =: b, \qquad 11.$$

with the mass difference $\Delta M_D = M_1 - M_2$ and the decay rate difference $\Delta\Gamma_D = \Gamma_1 - \Gamma_2$ of the mass eigenstates of the neutral D mesons. The mass difference is by definition positive, while the decay rate difference can have any sign; below, we specify only the positive one. The box diagrams that give rise to D mixing can have internal d, s, and b quarks, to be compared to u, c, and t, in the B sector (see **Figure 1**). M_{12}^D denotes the dispersive part of the box diagram, and Γ_{12}^D denotes the absorptive part; the relative phase of the two is given by $\phi_{12}^D = \arg(-M_{12}^D/\Gamma_{12}^D)$. Unlike in the B system, where $|\Gamma_{12}/M_{12}| \ll 1$ holds, the expressions for ΔM_D and $\Delta\Gamma_D$ in terms of M_{12}^D and Γ_{12}^D cannot be simplified, and to know ΔM_D, both M_{12}^D and Γ_{12}^D have to be determined. In general,

we get

$$\Delta\Gamma_D = \sqrt{2\left(\sqrt{a^2+b^2}-a\right)}, \quad \Delta M_D = \sqrt{\frac{\sqrt{a^2+b^2}+a}{2}}. \tag{12.}$$

However, it is well known that bounds like $|\Delta\Gamma_D| \leq 2|\Gamma_{12}^D|$ and $\Delta M_D \leq 2|M_{12}^D|$ hold generally for any values of M_{12}^D and Γ_{12}^D (28, 29). Experimental studies of charm mixing are sensitive to the parameters

$$x \equiv \frac{\Delta M_D}{\Gamma_D}, y \equiv \frac{\Delta\Gamma_D}{2\Gamma_D}, \tag{13.}$$

where Γ_D denotes the total decay rate of the neutral D mesons. Measurements (whose combined results are summarized later in Equation 36) show $y \sim 1\%$ and clearly establish the existence of a finite width difference in the neutral charm system. Current indications are that x has a similar value, although the possibility of having a vanishing mass difference is still not excluded.

However, if one assumes a small *CP*-violating phase ϕ_{12}^D, one obtains

$$\Delta\Gamma_D = 2|\Gamma_{12}^D|\left\{1 - \frac{4}{4+r}\frac{(\phi_{12}^D)^2}{2} + \mathcal{O}\left[(\phi_{12}^D)^4\right]\right\}, \tag{14.}$$

$$\Delta M_D = 2|M_{12}^D|\left\{1 - \frac{r}{4+r}\frac{(\phi_{12}^D)^2}{2} + \mathcal{O}\left[(\phi_{12}^D)^4\right]\right\}, \tag{15.}$$

with $r = |\Gamma_{12}^D|^2/|M_{12}^D|^2$. Note that the ratios $4/(4+r)$ and $r/(4+r)$ can vary only between zero and one, for any value of r. Thus, for values up to $\phi_{12}^D \approx 0.45 \approx 25^\circ$, the corrections due to the weak phase in Equations 14 and 15 are less than 10% and therefore clearly small compared with the theoretical precision. Using the approximations from Equations 14 and 15, experiment indicates that $r \approx 4y^2/x^2 \approx (13.5^{+16}_{-6})$. This is in stark contrast to the B system, where we have $r \approx 2 \times 10^{-5}$.

In the literature, "theoretical" mixing parameters are commonly defined as

$$x_{12} = 2\frac{|M_{12}^D|}{\Gamma_D}, \qquad y_{12} = \frac{|\Gamma_{12}^D|}{\Gamma_D}, \tag{16.}$$

which coincide with x and y up to corrections of order $(\phi_{12}^D)^2$.

Time-dependent *CP* asymmetries of neutral D meson decays into a *CP* eigenstate f (e.g., K^+K^-, $\pi^+\pi^-$) with eigenvalue η_{CP} depend on the quantity

$$\lambda_f = \frac{q}{p}\frac{\bar{A}_f}{A_f} = -\eta_{CP}\left|\frac{q}{p}\right| e^{i\phi^D}, \tag{17.}$$

where penguin corrections have been neglected (see, e.g., Reference 30). Here ϕ^D is the relative weak phase between the mixing contribution and the decay amplitudes. In the case of non-*CP* eigenstates, an additional strong phase will arise. Neglecting subleading CKM structures, the authors of Reference 30 find a relation between ϕ^D and ϕ_{12}^D:

$$\tan 2\phi^D = -\frac{\sin 2\phi_{12}^D}{\cos 2\phi_{12}^D + \frac{r}{4}} \rightarrow \phi^D \approx -\frac{4}{4+r}\phi_{12}^D + \mathcal{O}\left[(\phi_{12}^D)^3\right] \approx (0.2 \pm 0.1)\,\phi_{12}^D. \tag{18.}$$

We have expanded in small values of ϕ_{12} and inserted the experimental central values of x and y. The ratio q/p is also obtained by the diagonalization of the mixing matrix[1]

$$\frac{q}{p} = -\frac{2(M_{12}^D)^* - i(\Gamma_{12}^D)^*}{\Delta M_D + \frac{i}{2}\Delta\Gamma_D} \text{ with } \left|\frac{q}{p}\right| = 1 - \frac{2\sqrt{r}}{4+r}\phi_{12}^D + \frac{2r}{(4+r)^2}(\phi_{12}^D)^2 + \mathcal{O}\left[(\phi_{12}^D)^3\right]. \quad 19.$$

In the experimental discussion below, we define the quantities y_{CP} (see Equation 32 and Reference 32) and A_Γ (see Equation 33 and Reference 33); neglecting direct *CP* violation and expressing them in terms of ϕ^D and p/q, they read

$$y_{CP} = \frac{y}{2}\left(\left|\frac{q}{p}\right| + \left|\frac{p}{q}\right|\right)\cos\phi^D - \frac{x}{2}\left(\left|\frac{q}{p}\right| - \left|\frac{p}{q}\right|\right)\sin\phi^D \quad 20.$$

$$A_\Gamma = \frac{y}{2}\left(\left|\frac{q}{p}\right| - \left|\frac{p}{q}\right|\right)\cos\phi^D - \frac{x}{2}\left(\left|\frac{q}{p}\right| + \left|\frac{p}{q}\right|\right)\sin\phi^D. \quad 21.$$

Expanding in the mixing phase ϕ_{12}^D, we find

$$y_{CP} = y_{12}\left\{1 - \frac{32(\phi_{12}^D)^2}{(4+r)^2} + \mathcal{O}\left[(\phi_{12}^D)^3\right]\right\} \approx y_{12}\left\{1 - (0.1 \pm 0.1)\,\phi_{12}^2 + \mathcal{O}\left[(\phi_{12}^D)^3\right]\right\}, \quad 22.$$

$$A_\Gamma = 2\frac{2x_{12} - \sqrt{r}y_{12}}{4+r}\phi_{12}^D + \mathcal{O}\left[(\phi_{12}^D)^3\right] \approx -2 \times 10^{-3}\phi_{12}^D + \mathcal{O}\left[(\phi_{12}^D)^3\right], \quad 23.$$

where we have inserted on the right-hand sides of the last two equations the estimated value of r.

Γ_{12}^D can be expressed in terms of on-shell box diagrams differing in the internal quarks: $(s\bar{s})$, $(s\bar{d})$, $(d\bar{s})$, and $(d\bar{d})$ (see **Figure 1**). Using CKM unitarity ($\lambda_d + \lambda_s + \lambda_b = 0$), one gets

$$\Gamma_{12}^D = -\lambda_s^2\left(\Gamma_{ss}^D - 2\Gamma_{sd}^D + \Gamma_{dd}^D\right) + 2\lambda_s\lambda_b\left(\Gamma_{sd}^D - \Gamma_{dd}^D\right) - \lambda_b^2\Gamma_{dd}^D. \quad 24.$$

Equation 24 shows a very pronounced CKM hierarchy (8, 9):

$$\lambda_s^2 = +4.79 \times 10^{-2} - 5.85 \times 10^{-7}\,i, \quad 25.$$

$$2\lambda_s\lambda_b = -6.61 \times 10^{-5} + 1.16 \times 10^{-5}\,i, \quad 26.$$

$$\lambda_b^2 = +2.21 \times 10^{-8} - 7.99 \times 10^{-9}\,i. \quad 27.$$

The CKM suppression of the second term in Equation 24 relative to the first one is roughly three orders of magnitude. A similar suppression is found for the third term compared with the second one. It is interesting to note that the second term has a significant phase. Moreover, in the exact $SU(3)_F$ limit, $\Gamma_{ss}^D = \Gamma_{sd}^D = \Gamma_{dd}^D$ holds and the first two terms vanish, and only the tiny contribution from the third term survives. Below, we discuss in more detail the GIM cancellations taking place in the first two terms of this expression. The determination of M_{12}^D also involves box diagrams with internal b quarks; in contrast to Γ_{12}^D, the dispersive part of the diagrams has now to be determined. Denoting the dispersive part of a box diagram with internal x and y quarks by M_{xy}^D and using again CKM unitarity, one gets the following structure:

$$M_{12}^D = \lambda_s^2\left[M_{ss}^D - 2M_{sd}^D + M_{dd}^D\right] + 2\lambda_s\lambda_b\left[M_{bs}^D - M_{bd}^D - M_{sd}^D + M_{dd}^D\right] + \lambda_b^2\left[M_{bb}^D - 2M_{bd}^D + M_{dd}^D\right]. \quad 28.$$

[1]Reference 31 uses a different convention and thus obtains different signs in the expansion in ϕ_{12}.

In the case of neutral B mesons, the third term (replacing b, s, and d with t, c, and u) is clearly dominant, while for charm the extreme CKM suppression of λ_b might be compensated by a less pronounced GIM cancellation (1), and so all three terms of Equation 28 must be considered.

4.2. Theoretical Approaches

For the theoretical determination of M_{12}^D and Γ_{12}^D, one can use a quark-level (inclusive) or a hadron-level (exclusive) description. We briefly review the status of both approaches.

4.2.1. Inclusive approach. The inclusive approach for Γ_{12}^D is based on the heavy quark expansion (HQE) (34–40), which works very well for the B system (41–43). Interestingly, the HQE can successfully explain the large lifetime ratio $\tau(D^+)/\tau(D^0)$ (43, 44) indicating an expansion parameter $\Lambda/m_c \approx 0.3$. Lifetimes have the advantage of being free from GIM cancellations, and to make statements concerning the convergence of the HQE in the charm system more sound, future experimental and theoretical studies of other charmed mesons and charmed baryon lifetimes will be necessary.

Considering only a single diagram contributing to Γ_{12}^D—for instance, with only internal $s\bar{s}$ quarks—the HQE predicts (the nonperturbative matrix elements of dimension 6 operators have been determined in References 43, 45–47) a value for y that is five times larger than the experimental result (48). However, if one applies HQE to the whole expression of Equation 24, one encounters huge GIM suppression and obtains a result about four to five orders of magnitude below experiment (49).

Given the success of the HQE in the B system (where the expansion parameter is only a factor of three smaller) and for D meson lifetimes, it appears unlikely that HQE simply fails by four orders of magnitude in charm mixing. Instead, the problem seems to be rooted in the severe GIM cancellations. Several solutions to this puzzle have been suggested in the literature. The first idea, studied in References 50–53, is a lifting of the GIM cancellation in the first and second terms of Equation 24 by higher terms in the HQE, thereby overcompensating for the Λ/m_c suppression. First estimates of the dimension 9 contribution in the HQE for D mixing (54) indicate an enhancement compared with the leading dimension 6 terms, but unfortunately not one large enough to explain the experimental value. Here a full theory determination of the HQE terms of dimensions 9 and 12 will provide further insight. It is interesting to note that the lifting of GIM cancellation in D mixing by higher orders in the HQE (50–53) could also yield a sizeable CP-violating phase in Γ_{12}^D, stemming from the second term on the right-hand side of Equation 24. According to Reference 53, values of up to 1% for ϕ_{12}^D currently cannot be excluded. Using Equation 23, such a bound corresponds to $|A_\Gamma^{\rm SM}| \leq 2 \times 10^{-5}$.

An alternative origin of the discrepancy could lie in hypothetical violations of quark–hadron duality. On the one hand, the success of the HQE in the bottom sector and in the lifetime of charmed mesons, where no GIM cancellations arise, seems to exclude huge duality-violation effects. On the other hand, D mixing might be more affected by duality violations than lifetimes because of the smaller number of hadronic states that contribute in oscillations. In Reference 29 it was shown that duality violations as low as 20% could be sufficient to explain the discrepancy between experiment and the HQE prediction.

It was pointed out in Reference 49 that the severe GIM cancellations in the HQE prediction arise only if one uses identical renormalization scales for box-diagram contributions related to internal $s\bar{s}$ ($d\bar{d}$) and $s\bar{d}$ ($d\bar{s}$) quark pairs. Since the intermediate hadrons corresponding to $\Gamma_{ss,sd,dd}^D$ have a net strangeness of either zero (e.g., $K^+K^-, \pi^+\pi^-$) or one (e.g., $K^+\pi^-, \pi^+K^-$), there seems to be no reason for having to choose the scales for these different states to be identical. Varying the renormalization scales independently, it is found that the HQE prediction also nicely encompasses

the experimental result for y. To some extent, this result indicates that taking identical renormalization scales for $\Gamma^D_{ss,sd,dd}$ in combination with the GIM cancellations implicitly assumes a precision of the individual contributions of the order of 10^{-5}, which is clearly not realistic. Here a further study of higher-order perturbative corrections may provide additional insights (for first steps in this direction, see References 55, 56).

All in all, there is still more work to be done to obtain a deeper understanding of the HQE prediction for Γ^D_{12}, but it is not unrealistic to hope that this approach may accommodate the measured values of the mixing parameters. Once a satisfactory inclusive theory prediction for Γ^D_{12} becomes available, one could next aim for a quark-level determination of M^D_{12}, or one could use dispersion relations as briefly discussed below. Having reliable predictions for both Γ^D_{12} and M^D_{12}, we shall then be able to predict with confidence the weak mixing-phase ϕ^D_{12}.

4.2.2. Exclusive approach. The exclusive approach (see, e.g., References 57–61) aims to determine M^D_{12} and Γ^D_{12} at the hadron level. A potential starting point is the expressions

$$\Gamma^D_{12} = \sum_n \rho_n \langle \bar{D}^0 | \mathcal{H}^{\Delta C=1}_{\text{eff}} | n \rangle \langle n | \mathcal{H}^{\Delta C=1}_{\text{eff}} | D^0 \rangle, \tag{29.}$$

$$M^D_{12} = \sum_n \langle \bar{D}^0 | \mathcal{H}^{\Delta C=2}_{\text{eff}} | D^0 \rangle + \mathcal{P} \sum_n \frac{\langle \bar{D}^0 | \mathcal{H}^{\Delta C=1}_{\text{eff}} | n \rangle \langle n | \mathcal{H}^{\Delta C=1}_{\text{eff}} | D^0 \rangle}{m_D^2 - E_n^2}, \tag{30.}$$

where n denotes all possible hadronic states into which both D^0 and $\bar{D}^0$ can decay, ρ_n is the density of the state n, and $\mathcal{P}$ is the principal value. Unfortunately, a first-principle calculation of the arising nonperturbative matrix elements is beyond our current abilities. Thus, one has to make simplifying assumptions, such as taking only the SU(3)_F-breaking effects due to phase space effects into account, while neglecting any other hadronic effects, like SU(3)_F-breaking in the matrix elements. Following this approach, the authors of Reference 59 find that y could naturally be of the order of a percent, in agreement with current measurements. In more detail, they observe that contributions within a given SU(3)_F multiplet tend to cancel among themselves, and multiparticle final states seem to give large contributions to mixing, while resonances close to the threshold are not very relevant. Although encouraging, such a treatment clearly does not allow one to draw strong conclusions about the existence of BSM effects in the scenario in which the measurement disagrees with these expectations. In References 60 and 61, this method was improved by using experimental input and by attempting to take into account additional dynamical effects beyond phase space. For example, in Reference 61 the factorization-assisted topological-amplitude approach was used for this purpose, leading to the result that two-particle final states can give a value of $y = (0.21 \pm 0.07)\%$, which might again indicate the importance of multiparticle final states.

The exclusive approach seems to naturally predict a magnitude for y in agreement with measurement. However, for this method to be considered a genuine SM prediction, further improved experimental input (strong phases and branching ratios), as well as a theoretical inclusion of additional SU(3)_F-breaking effects, is necessary. On a very long timescale, it might become possible, through building on methods described in Reference 62, to use direct lattice calculations to predict the SM values for D mixing.

4.2.3. Dispersion relation. A dispersive relation between x and y was derived in Reference 63 in the heavy quark limit:

$$\Delta M_D = -\frac{1}{2\pi} \mathcal{P} \int_{2m_\pi}^{\infty} \mathrm{d}E \left[\frac{\Delta \Gamma_D(E)}{E - M_D} + \mathcal{O}\left(\frac{\Lambda_{\text{QCD}}}{E} \right) \right]. \tag{31.}$$

The authors conclude that if y is in the ballpark of +1%, then one expects x to be in the range of 10^{-3} to 10^{-2}, again in agreement with current measurements. Very recently, this dispersion relation, in combination with additional assumptions, has been used to derive bounds on *CP* violation in D mixing (64).

4.3. Experiment

The existence of charm mixing was first established in 2007 by combining the ensemble of results from the *B* factories, CDF, and earlier experiments (65). The first single-experiment observation was made by the LHCb Collaboration in 2013 (66) and was followed by CDF and Belle soon after (10, 13).

Mixing studies may be divided into three main categories: measurements of decays into *CP* eigenstates, measurements of decays into flavor eigenstates, and analyses of multibody self-conjugate modes that account for the position of the decay in phase space.

4.3.1. Measurements with *CP* eigenstates. Charm mixing in D^0 decays to *CP* eigenstates of eigenvalue η_{CP} gives rise to an effective lifetime τ_{CP}, which differs from that in decays to flavor-specific states, $\tau_{\rm FS}$. The observable

$$y_{CP} \equiv \eta_{CP}\left(\frac{\tau_{\rm FS}}{\tau_{CP}} - 1\right) \qquad 32.$$

is equal to y in the limit of *CP* conservation and more generally is given by Equation 20. When allowing for direct *CP* violation, specific to mode f with decay amplitude A_f, Equation 20 receives an additional contribution of $(A_D^f/2)x\sin\phi^D$, with $A_D^f \equiv |A_f/\bar{A}_f|^2 - 1$.

Valuable information may also be gained from studying the time-dependent asymmetry

$$A_{CP}(f;t) \equiv \frac{\Gamma\left(D^0(t)\to f\right) - \Gamma\left(\bar{D}^0(t)\to f\right)}{\Gamma\left(D^0(t)\to f\right) + \Gamma\left(\bar{D}^0(t)\to f\right)}, \qquad 33.$$

which in the case of *CP* violation has an approximate linear dependence

$$A_{CP}(f;t) \approx a_{CP}^{\rm dir}(f) - A_\Gamma(f)\frac{t}{\tau}, \qquad 34.$$

driven by a potential direct *CP*-violating asymmetry $a_{CP}^{\rm dir}(f)$ and a second parameter, $A_\Gamma(f)$. When direct *CP* violation is neglected, the latter contribution is universal and is given by Equation 21; otherwise, this expression receives an offset of $-ya_{CP}^{\rm dir}(f)$.

Measurements of y_{CP} and A_Γ have been performed by several experiments, usually exploiting the decays $D^0 \to K^+K^-$ and $D^0 \to \pi^+\pi^-$. A selection of the most precise results is presented in **Table 2**. With current sensitivity, there is no indication of a difference between $A_\Gamma(K^+K^-)$ and $A_\Gamma(\pi^+\pi^-)$, so the results are combined to yield a universal observable. **Figure 2** shows the ratio of the lifetime distributions of $D^0 \to K^+K^-$ to $D^0 \to K^-\pi^+$, and $D^0 \to \pi^+\pi^-$ to $D^0 \to K^-\pi^+$ from Reference 67 in which the nonzero slope is clearly evident.

The measurement of y_{CP} in a hadron collider is challenging. The trigger generally introduces a decay time–dependent acceptance that is not identical for $D^0 \to K^+K^-$, $\pi^+\pi^-$, and $K^-\pi^+$ because of the different masses of the decay products. The most precise measurement to emerge so far from LHCb is for semileptonically tagged decays with Run 1 data, where this problem is less acute, but for which the statistical and systematic uncertainties are still of a similar magnitude. Currently, y_{CP} is measured with a precision of 0.11% and is compatible with the measurements of y from other methods.

Table 2 Selected results for y_{CP} and A_Γ

Measurement	y_{CP} (%)	Measurement	A_Γ (%)
Belle, 673 fb^{-1} (68)	$0.11 \pm 0.61 \pm 0.52$	Belle, 976 fb^{-1} (69)	$-0.03 \pm 0.20 \pm 0.07$
Belle, 976 fb^{-1} (69)	$1.11 \pm 0.22 \pm 0.09$	CDF, 9.7 fb^{-1} (70)	-0.12 ± 0.12
BaBar, 468 fb^{-1} (71)	$0.72 \pm 0.18 \pm 0.12$	LHCb D^{*+}, 3 fb^{-1} (72)	$-0.013 \pm 0.028 \pm 0.010$
LHCb SL, 3 fb^{-1} (67)	$0.57 \pm 0.13 \pm 0.09$	LHCb SL, 5.4 fb^{-1} (73)	$-0.029 \pm 0.032 \pm 0.004$
World average (65)	0.72 ± 0.11	World average (65)	-0.031 ± 0.020

All values derive from the combination of $D^0 \to K^+K^-$ and $\pi^+\pi^-$, apart from those taken from Reference 68, which is from $D^0 \to K^0_S K^+K^-$. The combination for Reference 73 has been made by the authors of this review. When two uncertainties are shown, they are statistical and systematic, respectively.

The determination of A_Γ is inherently robust because an asymmetry measurement involves the same final state, and the parameter of interest is the slope of the asymmetry, which can be biased only by time-dependent systematic effects in the tagging process, residual backgrounds, or secondary contamination. The experimental picture is now wholly dominated by LHCb measurements, which themselves are limited by the statistical uncertainties. The measurement procedure is validated by determining a "pseudo A_Γ" with the CF $D^0 \to D^-\pi^+$ decay, where negligible *CP* violation, and hence a result of zero, is expected. Self-consistency is also required over all running periods, in particular between those of opposite dipole polarity. The current world average for A_Γ is compatible with *CP* conservation and is measured with a precision of 2×10^{-4}, which makes it one of the best-known quantities in flavor physics. Significant near-term improvements can be expected from the analysis of the LHCb Run 2 prompt sample.

Other decay modes can be harnessed for these measurements. The Belle Collaboration has studied the *CP*-odd channel $D^0 \to K^0_S\omega$ (74) and also has performed a measurement that compares the time evolution of different regions of the Dalitz plot for the decay $D^0 \to K^0_S K^+K^-$ (68). It has been proposed that self-conjugate channels such as $D^0 \to \pi^+\pi^-\pi^0$ can also be exploited in an

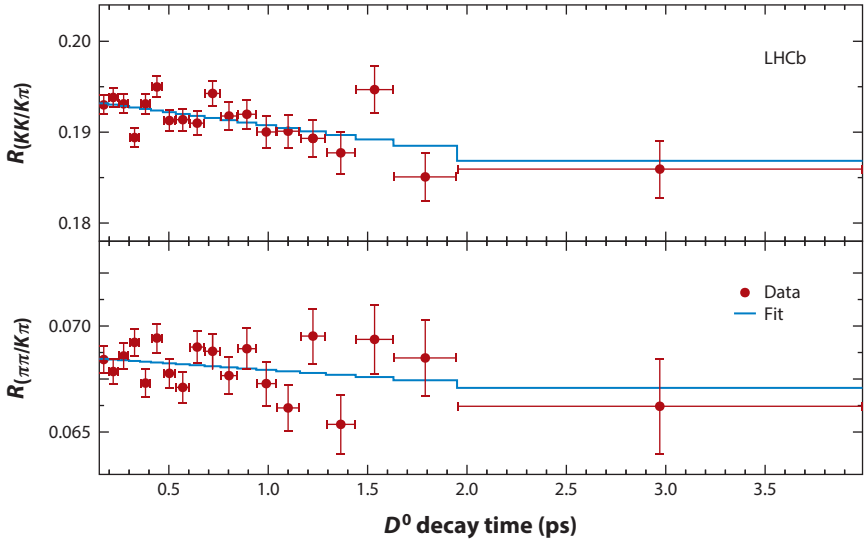

Figure 2

Ratio of the lifetime distributions of $D^0 \to K^+K^-$ to $D^0 \to K^-\pi^+$ and $D^0 \to \pi^+\pi^-$ to $D^0 \to K^-\pi^+$ decays. Figure adapted from Reference 67 (CC BY 4.0).

Table 3 Results, assuming *CP* conservation, of the effective mixing parameters from selected measurements of the time-dependent $D^0 \to K^+\pi^-$ to $D^0 \to K^-\pi^+$ ratio performed at the *B* factories, the Tevatron, and the LHC

	y' (%)	x'^2 (10^{-3})	Reference
Belle, 976 fb^{-1}	0.46 ± 0.34	0.09 ± 0.22	10
CDF, 9.6 fb^{-1}	0.43 ± 0.43	0.08 ± 0.18	13
LHCb D^{*+}, 5.0 fb^{-1}	$0.528 \pm 0.045 \pm 0.027$	$0.039 \pm 0.023 \pm 0.014$	15

When two uncertainties are shown, they are statistical and systematic, respectively.

inclusive manner, provided their net *CP* content is known (75). Modes such as $D^0 \to K^0_S\pi^0$ are unsuitable, even at *B* factories, because of the poor resolution on the proper time.

4.3.2. Measurements with flavor eigenstates. Decays into flavor-specific final states, in particular those that can be accessed by both CF and DCS amplitudes, play a central role in charm-mixing analyses. The most studied of these channels is the so-called wrong-sign decay $D^0 \to K^+\pi^-$, to be distinguished from the right-sign decay $D^0 \to K^-\pi^+$.

In the absence of *CP* violation, the time-dependent ratio between wrong-sign and right-sign decays is

$$R(t/\tau) \approx R_D + \sqrt{R_D}y'(t/\tau) + \frac{x'^2 + y'^2}{4}(t/\tau)^2. \qquad 35.$$

Here the first term, $R_D \approx 0.34\%$, is the squared ratio of the DCS to CF amplitudes, the second term arises from interference between the mixing and the DCS amplitudes, and the final term is generated by the mixing amplitude alone. The rotated mixing parameters are $x' = x\cos\delta + y\sin\delta$ and $y' = y\cos\delta - x\sin\delta$, where δ is the strong-phase difference between the CF and DCS amplitudes, the value of which must be known to interpret the results in terms of the mixing parameters. Although this strong-phase difference may be measured in quantum-correlated decays at charm threshold, the uncertainty on our current knowledge, $\delta = (16.1^{+7.9}_{-10.1})^\circ$, is essentially set by a global fit to all charm-mixing measurements (65). Future analyses exploiting larger $\psi(3770)$ data sets, and overconstrained fits to *b* physics measurements made for the purpose of determining the Unitarity Angle γ, which also exploit this charm decay, will help to improve the precision on the strong-phase difference.

The analysis may be extended to probe for *CP* violation by measuring $R(t/\tau)^+$ and $R(t/\tau)^-$, the separate ratios for D^0 and $\bar{D}^0$ decays, respectively. Direct *CP* violation, here expected to be negligible in the SM, would generate different values of the offset, and indirect *CP* violation would change the time-dependent terms, with $x'^{\pm} = |q/p|^{\pm 1}(x'\cos\phi^D \pm y'\sin\phi^D)$ and $y'^{\pm} = |q/p|^{\pm 1}(y'\cos\phi^D \mp x'\sin\phi^D)$.

Results from selected measurements of the effective mixing parameters are shown in **Table 3**. The most precise study, from which the $R(t/\tau)$ distributions are shown in **Figure 3**, is still limited by the statistical uncertainty (15). The dominant systematic uncertainties are determined from the data themselves and, therefore, are expected to decrease with future measurements. For example, the wrong-sign sample suffers contamination from right-sign decays in which the kaon is misidentified as a pion, and the pion as a kaon. Knowledge of the magnitude of this background is limited by the understanding of the particle-identification performance, which is studied using control samples in data. The parameter y' is currently measured with a precision of about 0.05%, and x'^2 is compatible with zero. Results of separate fits to $R^+(t/\tau)$ and $R^-(t/\tau)$ are consistent with *CP* conservation.

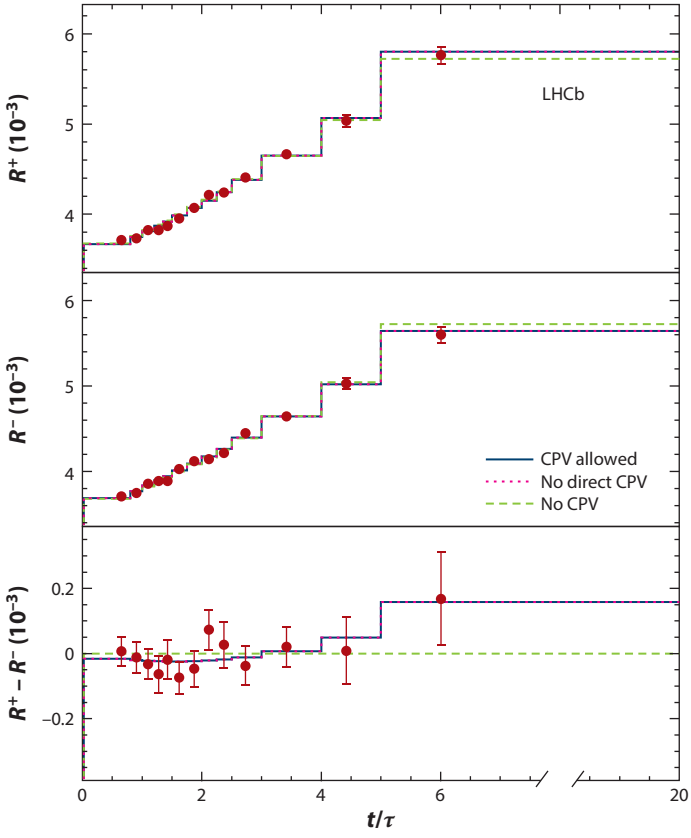

Figure 3

The ratio $R(t/\tau)$ in the $K\pi$ mixing analysis, shown for D^0- and $\bar{D}^0$-tagged decays (R^+ and R^-, respectively), and the difference between them. Various fit hypotheses are superimposed. Abbreviation: CPV, *CP* violation. Figure adapted from Reference 15 (CC BY 4.0).

It is possible to analyze multibody CF/DCS decays, such as $D^0 \to K^{\mp}\pi^{\pm}\pi^+\pi^-$ and $D^0 \to K^{\mp}\pi^{\pm}\pi^0$, in a similar fashion. In this case, however, the interpretation of the time-dependent wrong-sign to right-sign ratio must account for the fact that the amplitude ratio and strong-phase difference vary over the phase space of the final-state particles. In an inclusive analysis, the equivalent parameters for R_D and δ are averaged over this phase space for the decay in question (76). Furthermore, the linear term in y' of Equation 35 is multiplied by a parameter called the coherence factor (77). The coherence factor takes a value between zero and unity and dilutes the mixing signature. Both the coherence factor and the average strong-phase difference can be determined at charm threshold (78, 79) and used to interpret the multibody mixing measurement in terms of x and y, as has been demonstrated in an LHCb study of $D^0 \to K^{\mp}\pi^{\pm}\pi^+\pi^-$ decays (80). The dilution and consequent loss of information that come with an inclusive analysis can be partially recovered through performing the measurement in bins of phase space (81). Full statistical sensitivity can be achieved by using models to track the continuous variation of the phase difference between CF and DCS amplitudes in an unbinned measurement, as was shown by the BaBar Collaboration in a study of $D^0 \to K^{\mp}\pi^{\pm}\pi^0$ decays (82). However, the systematic uncertainty arising from imperfections in the models is very difficult to assess, rendering this approach unsatisfactory for precision studies.

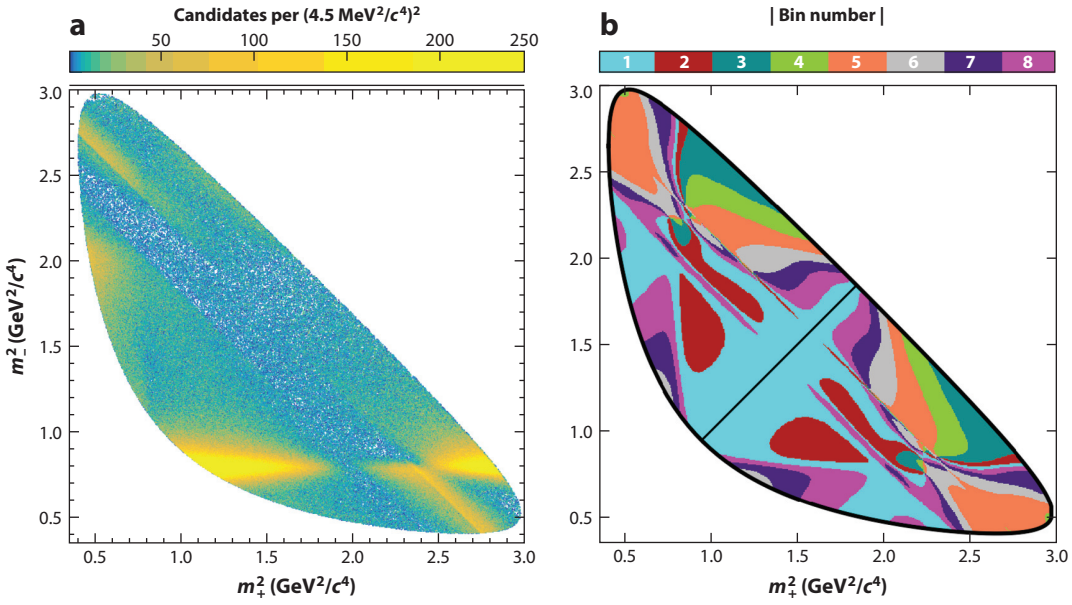

Figure 4

Dalitz plot of $D^0 \to K^0_S\pi^+\pi^-$ decays, with $m^2_\pm = m^2(K^0_S\pi^\pm)$. (*a*) Distribution of data (17). (*b*) Bins of equal-interval strong-phase difference as defined in Reference 84.

4.3.3. Measurements with multibody self-conjugate decays. As is evident from its Dalitz plot (**Figure 4*a***), the mode $D^0 \to K^0_S\pi^+\pi^-$ has a rich resonance structure. The decay receives contributions both from *CP* eigenstates, such as $D^0 \to K^0_S\rho^0$, and from flavor eigenstates, such as $D^0 \to K^{*\mp}\pi^\pm$. Hence, as first pointed out in Reference 83, an analysis that pays attention to the position of each decay in phase space can be considered as a combination of the two strategies discussed above. Moreover, the strong-phase difference varies over the Dalitz plot, ensuring that the analysis has greater sensitivity to the parameter x than in the case of $D^0 \to K^\mp\pi^\pm$ decays. The measurement may be performed separately for D^0 and $\bar{D}^0$ mesons to probe for *CP* violation. There is sufficient information in the Dalitz plot to allow a simultaneous fit of x, y, ϕ^D, and $|q/p|$, giving $D^0 \to K^0_S\pi^+\pi^-$ a particularly important role in charm studies.

Knowledge of the strong-phase variation is available from two alternative sources, following similar considerations to those discussed for multibody decays in Section 4.3.2. First, an amplitude model may be constructed from a fit to the time-integrated Dalitz plot to describe the contribution of each resonance and the interference between them. A second approach is to use charm-threshold data to measure the mean strong-phase difference (or, in practice, the amplitude-weighted cosine and sine of this quantity) in bins of phase space. The definition of these bins is itself guided by amplitude models. **Figure 4*b*** shows one such partitioning of the Dalitz plot, in which eight pairs of symmetrical bins are chosen. The bin boundaries separate the expected phase difference into intervals of $2\pi/8$ radians. Measurements of the strong-phase difference within these bins have been performed by both the CLEO and BESIII Collaborations (22, 84).

The mixing analysis is performed either through an unbinned fit of the data set that assumes the amplitude variation given by the model or through a binned analysis that makes use of the charm-threshold inputs (85, 86). The latter strategy has the benefit of incurring no model dependence, at the expense of some loss of statistical sensitivity. At hadron collider experiments, the trigger can

Table 4 Results for the mixing and the *CP*-violation parameters from $D^0 \to K^0_S\pi^+\pi^-$ decays

	Belle, 540 fb^{-1} (89)	BaBar, 469 fb^{-1} (88)	LHCb D^{*+} and SL, 3.0 fb^{-1} (17)
x (%)	$0.81^{+0.33}_{-0.35}$	0.16 ± 0.27	$0.27^{+0.17}_{-0.15}$
y (%)	$0.37^{+0.27}_{-0.29}$	0.57 ± 0.25	0.74 ± 0.37
ϕ^D (°)	-14^{+17}_{-18}	NM	$-5.2^{+6.3}_{-9.2}$
$\lvert q/p\rvert$	$0.86^{+0.32}_{-0.30}$	NM	$1.05^{+0.22}_{-0.17}$

The results from Reference 88 also include input from $D^0 \to K^0_S K^+K^-$.
Abbreviation: NM, not measured.

induce significant acceptance variations over the Dalitz plot, which may also have a dependence on proper time. To ameliorate this problem, a modified version of the model-independent binned analysis has been proposed, in which ratios of yields are constructed in pairs of symmetric bins, much like the $R(t/\tau)$ ratio of Equation 35. This bin-flip method is experimentally robust and also has the consequence of enhancing sensitivity to the less well-known mixing parameter x, albeit at the expense of degrading sensitivity to y (87).

Results are shown in **Table 4** for model-dependent analyses from the B factories and a model-independent bin-flip analysis from LHCb. The sample size exploited in the LHCb measurement is around 2.3 million decays, approximately four times that of each of the B-factory studies. This analysis provides the single most precise determination of the parameter x. The systematic uncertainties on the mixing parameters are around a quarter of the statistical uncertainties and are dominated by the finite knowledge of the strong-phase information, which in this study comes from Reference 84 alone. Other self-conjugate multibody decays that have been exploited for charm-mixing measurements include $D^0 \to K^0_S K^+K^-$ (88) and $D^0 \to \pi^+\pi^-\pi^0$ (11).

4.3.4. Summary of current knowledge and experimental prospects. Fits are performed to the ensemble of charm-mixing data by the HFLAV group (65), with the most recent results dating from July 2020. The central values and 1σ uncertainties on the mixing parameters are

$$x = (0.37 \pm 0.12)\%, \quad y = 0.68^{+0.06}_{-0.07}\%,$$
$$|q/p| = 0.951^{+0.053}_{-0.042}, \quad \phi^D = (-5.3^{+4.9}_{-4.5})^\circ, \qquad 36.$$

and the 1σ to 5σ contours are displayed in **Figure 5**. In summary, y is well measured, but a nonzero value of x has not been excluded. The measurements do not yet have sufficient sensitivity to approach the SM expectation for *CP* violation, but they already confirm that any effects are small.

Steady progress can be expected over the coming two decades. A complete set of analyses based on the full Run 1 and 2 LHCb data sets will bring a significant increase in sensitivity. The samples will grow by an order of magnitude at Upgrade I of LHCb, and important measurements will soon arrive from Belle II. At LHCb Upgrade II, the statistical uncertainties on $|q/p|$ and ϕ^D are expected to shrink to 0.004 and 0.18°, respectively, from the $D^0 \to K^0_S\pi^+\pi^-$ analysis alone (19). The challenge will be to attain sufficient experimental control to match these advances in statistical precision. It also will be necessary to improve the measurements of strong-phase parameters (e.g., at a Super Tau Charm Factory), although it will become possible to fit these parameters with reasonable sensitivity as part of the next generation of LHCb and Belle II analyses.

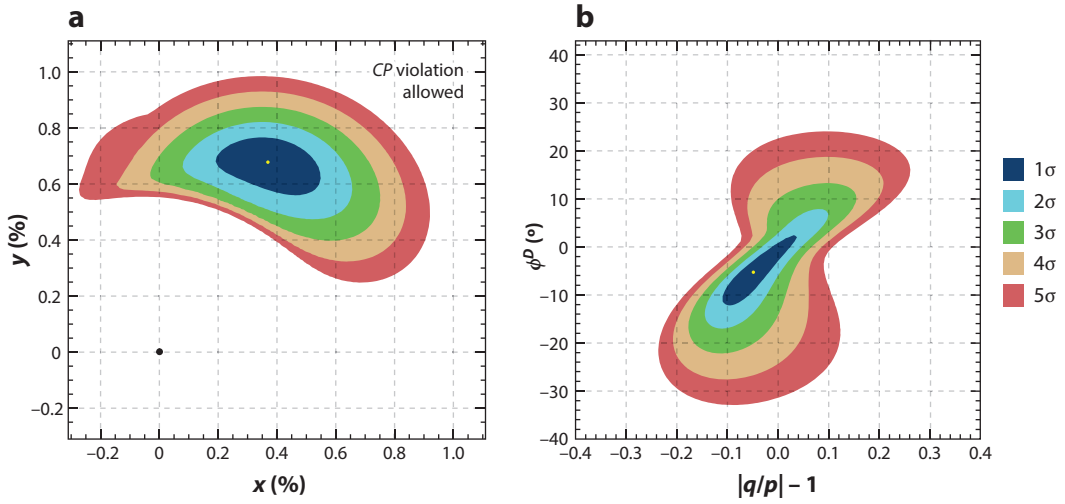

Figure 5

Contours for (*a*) the mixing parameters x and y and (*b*) the *CP*-violation parameters ϕ^D and $|q/p| - 1$. Figure adapted from online update to Reference 65 (**https://hflav.web.cern.ch**).

4.4. Bounds on BSM Models from *D* Mixing

Because of its pronounced SM suppression, *D* mixing is particularly suited for indirect searches for BSM effects. This attribute is exploited in Reference 90, in which a wide class of New Physics models is discussed. Assuming an off-diagonal tree-level coupling of some BSM mediator to the neutral *D* meson, one can test BSM scales higher than 10^4 TeV (see, e.g., Reference 91 based on Reference 92). It is common in such BSM studies to neglect the SM contribution to *D* mixing and to saturate the experimental results completely by the BSM contribution. Without doubt, *D*-mixing measurements give very stringent constraints on any BSM model that acts in the charm sector, as is also stressed below in Section 5.3.2 in the context of direct *CP* violation.

5. DIRECT *CP* VIOLATION IN SINGLY CABIBBO-SUPPRESSED DECAYS

The most promising avenue to search for direct *CP* violation in charm is through the study of SCS decays, given the contribution of penguin diagrams to these processes. Although not discussed further in this review, it should be stressed that CF and DCS decays are also of interest, as any signal of direct *CP* violation here would be a clear sign of BSM effects. Another worthwhile area of investigation is the study of *CP*-violating effects in flavor-changing neutral-current charm decays, as discussed in References 93 and 94, but that topic is beyond the scope of this review.

In this section, we briefly review the status of two-body SCS *CP*-asymmetry measurements and the experimental challenges that these entail and then focus in more detail on the determination and interpretation of ΔA_{CP}, the difference in the time-integrated *CP* asymmetries of $D^0 \to K^+K^-$ and $D^0 \to \pi^+\pi^-$. We then give a summary of the methods and status of *CP* studies of multibody SCS decays. We conclude with some remarks on *CP*-violation measurements in the charm baryon sector.

5.1. Measuring the *CP* Asymmetry and Studies of Two-Body Decays

For charged mesons and baryons, the *CP* asymmetry $A_{CP}(f)$ is the time-independent form of Equation 33, with f now not restricted to *CP* eigenstates, and $A_{CP}(f) = a_{\rm dir}(f)$, which is the direct

CP asymmetry for the mode in question. For neutral mesons, $A_{CP}(f)$ is integrated with respect to proper time and, in addition to $a_{\rm dir}$, receives a contribution from indirect *CP* violation.

In general, the measured asymmetry $A_{\rm raw}(f)$ does not exactly correspond to the underlying physics asymmetry, as it can be biased by several detector- and facility-related effects. In the case that the *CP* asymmetry and these effects are small, then

$$A_{\rm raw}(f) = A_{CP}(f) + a_{\rm det}(f) + a_{\rm tag}(f) + a_{\rm prod}(f). \quad 37.$$

Here, $a_{\rm det}(f)$ is the detection asymmetry for final state f, which can be nonzero for any decay apart from those into a *CP* eigenstate involving pseudoscalars. Contributions to $a_{\rm det}(f)$ come from, for example, differences in trigger or reconstruction efficiency for positive and negative particles, or from the different interaction cross sections in the detector material for kaons with positive and negative strangeness. The tagging asymmetry $a_{\rm tag}(f)$ applies only for measurements with neutral mesons and is driven by different detection efficiencies for the slow pion or lepton tags. Although these effects are independent of the final state f, correlations can occur through the acceptance of the detector. Finally, the pp initial state at the LHC can lead to a production asymmetry $a_{\rm prod}(f)$ with different proportions of hadrons of each flavor produced within the detector acceptance. Again, correlations induced by detector acceptance effects can result in the effective value of this asymmetry acquiring a dependence on the final state. Typically, $a_{\rm det}(f)$, $a_{\rm tag}(f)$, and $a_{\rm prod}(f)$ are all $\mathcal{O}(\%)$, which is larger than the expected value of $A_{CP}(f)$.

When measuring A_{CP} for an SCS decay, it is customary to use CF control channels to account for the detection, tagging, and production asymmetries. Negligible *CP* violation is expected for these modes; that is, any nonzero raw asymmetry must arise from the other sources. For example, in the D^{*+}-tagged determination of $A_{CP}(K^+K^-)$ at LHCb measurements of the raw asymmetries of the modes $D^0 \to K^-\pi^+$, $D^+ \to K^-\pi^+\pi^+$ and $D^+ \to \bar{K}^0\pi^+$ are employed to subtract the detection and production asymmetries (95). These asymmetries are measured after reweighting the kinematics of the control samples so that they match those of the quantities they are being used to describe. Furthermore, fiducial cuts are applied to exclude regions of the acceptance where detector asymmetries are known to be large. Finally, a small correction must be made for cross section interaction effects, mixing, and *CP* violation for the neutral kaon in the third control mode, but this may be calculated with excellent precision.

Table 5 lists the most precise individual measurements of the *CP* asymmetries for SCS decays of D^0, D^+, and D_s^+ mesons into two-body final states involving pions and kaons [note that a more precise determination of $A_{CP}(\pi^+\pi^-)$ can be obtained through a combination of $A_{CP}(K^+K^-)$ and the

Table 5 Most precise individual measurements of A_{CP} in two-body singly Cabibbo-suppressed decays

Mode	A_{CP} (%)	Experiment	Reference
$D^0 \to \pi^+\pi^-$	$+0.22 \pm 0.24 \pm 0.11$	CDF, 5.9 fb^{-1}	96
$D^0 \to K^+K^-$	$+0.14 \pm 0.15 \pm 0.10$	LHCb D^{*+} and SL, 3.0 fb^{-1}	95
$D^0 \to \pi^0\pi^0$	$-0.03 \pm 0.64 \pm 0.10$	Belle, 966 fb^{-1}	97
$D^0 \to K_S^0K_S^0$	$-0.02 \pm 1.53 \pm 0.17$	Belle, 921 fb^{-1}	98
$D^+ \to \pi^+\pi^0$	$+2.31 \pm 1.24 \pm 0.23$	Belle, 921 fb^{-1}	99
$D^+ \to K_S^0K^+$	$-0.009 \pm 0.065 \pm 0.048$	LHCb, 3.8 fb^{-1}	100
$D_s^+ \to K^+\pi^0$	$-26.6 \pm 23.8 \pm 0.9$	CLEO, 586 nb^{-1}	101
$D_s^+ \to K_S^0\pi^+$	$+0.13 \pm 0.19 \pm 0.05$	LHCb, 3.8 fb^{-1}	100

The measurements from Reference 100 are corrected for the effects of *CP* violation in the neutral kaon system. The uncertainties are statistical and systematic, respectively.

ΔA_{CP} measurement, as discussed in Section 5.2]. All results are compatible with *CP* conservation. The precision of these measurements is expected to improve with the analysis of larger samples, as many of the contributions to the systematic uncertainties are directly determined from the data themselves.

5.2. The Measurement of ΔA_{CP}

The quantity $\Delta A_{CP} \equiv A_{CP}(K^+K^-) - A_{CP}(\pi^+\pi^-)$ can be measured with very small systematic uncertainty. If the variation in acceptance of both decays is the same—an assumption that can be made valid by reweighting the kinematics of the two samples to agree—then the tagging and production asymmetries of the decays are also identical, and so $\Delta A_{CP} = A_{\rm raw}(K^+K^-) - A_{\rm raw}(\pi^+\pi^-)$.

The LHCb Collaboration has performed this measurement with 5.9 fb^{-1} of data collected in Run 2 using both D^{*+} and semileptonic tags (102), and obtained

$$\Delta A_{CP}\,(D^{*+}) = \left[-18.2 \pm 3.2\,(\text{stat.}) \pm 0.9\,(\text{syst.})\right] \times 10^{-4}$$
$$\Delta A_{CP}\,(\text{SL}) = \left[-9 \pm 8\,(\text{stat.}) \pm 5\,(\text{syst.})\right] \times 10^{-4},$$

which can be combined with measurements made with 3.0 fb^{-1} of data from Run 1 (103, 104) to give

$$\Delta A_{CP} = (-15.4 \pm 2.9) \times 10^{-4}. \qquad 38.$$

The significance of the deviation from zero is 5.3 standard deviations, and hence this measurement constitutes the first observation of *CP* violation in charm decays. It is instructive to note the enormous samples required for this important result: around 51 million D^{*+}-tagged $D^0 \to K^+K^-$ decays and 11 million D^{*+}-tagged $D^0 \to \pi^+\pi^-$ decays, and around 11 million semileptonic $D^0 \to K^+K^-$ decays and 4 million semileptonic $D^0 \to \pi^+\pi^-$ decays.

Because of the presence of mixing, there is the possibility of a contribution from indirect *CP* violation to the individual asymmetries. Therefore,

$$\Delta A_{CP} = \Delta a_{\rm dir} - \frac{\Delta\langle t\rangle}{\tau} A_\Gamma, \qquad 39.$$

where $\Delta a_{\rm dir}$ is the difference in direct *CP* asymmetries between the two decays, $\Delta\langle t\rangle$ is the difference in the mean decay times of the two decays in the analysis, and τ is the D^0 lifetime. This expression assumes that the indirect *CP* violation, manifested through A_Γ, is the same for the two decays. It is then found that

$$\Delta a_{\rm dir} = (-15.7 \pm 2.9) \times 10^{-4}, \qquad 40.$$

indicating that ΔA_{CP} is primarily sensitive to direct *CP* violation, and the direct *CP* asymmetries are different for the two decays.

There are no known irreducible systematic uncertainties in the ΔA_{CP} measurement, so significant improvements in knowledge can be expected at LHCb over the coming years; the statistical precision after Upgrade II is predicted to be an order of magnitude better than at present (19). It is naturally of great interest to know the values of the individual asymmetries, and an improved measurement of $A_{CP}(K^+K^-)$ is eagerly awaited from the full Run 2 data set. Most likely, however, data from Run 3 will be required to establish a nonzero asymmetry for either decay. The final sample sizes at Belle II for the two modes will be smaller than those already accumulated by LHCb; however, measurements performed there will be valuable because of the very different experimental environment.

5.3. Theory for ΔA_{CP}

The amplitude of the SCS decay $D^0 \to \pi^+\pi^-$ can be decomposed as

$$A(D^0 \to \pi^+\pi^-) = \lambda_d \left(A_{\text{tree}} + A^d_{\text{peng}}\right) + \lambda_s A^s_{\text{peng}} + \lambda_b A^b_{\text{peng}}, \tag{41.}$$

with a tree-level amplitude A_{tree} accompanied by the CKM structure λ_d and three penguin contributions A^q_{peng} with the internal quark $q = d, s, b$ and the CKM structure λ_q. Using the unitarity of the CKM matrix, all additional, more complicated contributions such as rescattering effects can be included in the same scheme to obtain

$$A(D^0 \to \pi^+\pi^-) = \frac{G_F}{\sqrt{2}} \lambda_d \, T \left[1 + \frac{\lambda_b}{\lambda_d} \frac{P}{T}\right]. \tag{42.}$$

Here, T contains not only pure tree-level contributions but also penguin topologies (P), weak exchange (E) insertions, and rescattering (R) effects, while P consists of tree insertion of penguin operators and penguin insertions of tree-level operators:

$$T = \sum_{i=1,2} C_i \langle Q^d_i \rangle^{T+P+E+R} - \sum_{i=1,2} C_i \langle Q^s_i \rangle^{P+R}, \; P = \sum_{i>3} C_i \langle Q^b_i \rangle^T - \sum_{i=1,2} C_i \langle Q^s_i \rangle^{P+R}. \tag{43.}$$

Physical observables—for example, branching ratios (Br) and direct CP asymmetries (a_{dir})—can be expressed in terms of $|T|$, $|P/T|$, and the strong phase $\Phi^S = \arg(P/T)$ as

$$\text{Br} \propto \frac{G_F^2}{2} |\lambda_d|^2 |T|^2 \left|1 + \frac{\lambda_b}{\lambda_d} \frac{P}{T}\right|^2 \approx \frac{G_F^2}{2} |\lambda_d|^2 |T|^2, \tag{44.}$$

$$a_{\text{dir}} = \frac{-2 \left|\frac{\lambda_b}{\lambda_d}\right| \sin\gamma \left|\frac{P}{T}\right| \sin\Phi^S}{1 - 2 \left|\frac{\lambda_b}{\lambda_d}\right| \cos\gamma \left|\frac{P}{T}\right| \cos\Phi^S + \left|\frac{\lambda_b}{\lambda_d}\right|^2 \left|\frac{P}{T}\right|^2} \approx -13 \times 10^{-4} \left|\frac{P}{T}\right| \sin\Phi^S. \tag{45.}$$

The approximations on the right-hand side are based on $|\lambda_b/\lambda_d| \approx 7 \times 10^{-4}$. For the $D^0 \to K^+K^-$ decay, the same formalism applies with obvious replacements, and we find (neglecting mixing-induced CP violation)

$$|\Delta A_{CP}| \approx 13 \times 10^{-4} \left| \left|\frac{P}{T}\right|_{K^+K^-} \sin\Phi^S_{K^+K^-} + \left|\frac{P}{T}\right|_{\pi^+\pi^-} \sin\Phi^S_{\pi^+\pi^-} \right|. \tag{46.}$$

To quantify the possible size of the direct CP violation, we need to know $|P/T|$ and the strong phase Φ^S for both decays. Since the branching ratios are well measured (105),

$$\text{Br}(D^0 \to K^+K^-) = 4.08 \pm 0.06 \times 10^{-3}, \; \text{Br}(D^0 \to \pi^+\pi^-) = 1.455 \pm 0.024 \times 10^{-3},$$

their values can be used to estimate the size of T via Equation 44. With this information, one can then determine an upper SM bound by maximizing the strong phase and using only a theory estimate for the size of P.

5.3.1. SM estimates. The magnitude of ΔA_{CP} is larger than would be predicted based on naive expectations, and it is currently unclear whether this value is governed by the SM or whether we are already seeing a first glimpse of BSM effects.

Naive perturbative estimates yield $|P/T| \approx 0.1$ (see, e.g., References 106–109), resulting in the upper bound

$$|\Delta A_{CP}| \approx \leq 2.6 \times 10^{-4}, \tag{47.}$$

which is roughly an order of magnitude smaller than what is observed.

Light-cone sum rules (LCSRs) (110) are a QCD-based method allowing the determination of hadronic matrix elements, including nonperturbative effects. This method has been used by the authors of Reference 111 to predict the *CP* asymmetries in neutral *D* meson decays. Extracting values of the matrix element $|T|$ from the experimental measurements of the branching ratios, the magnitudes and phases of *P* are then determined with LCSRs. In that study, no prediction is made of the relative strong phase between the tree-level *T* and penguin *P* contributions, which therefore remains a free parameter. This calculation has been numerically updated in Reference 112 and yields

$$\left|\frac{P}{T}\right|_{\pi^+\pi^-} = 0.093 \pm 0.056, \left|\frac{P}{T}\right|_{K^+K^-} = 0.075 \pm 0.048, \tag{48.}$$

which gives an SM bound for ΔA_{CP} of

$$|\Delta A_{CP}| \leq (2.2 \pm 1.4) \times 10^{-4} \leq 3.6 \times 10^{-4}. \tag{49.}$$

It is interesting to note that this result agrees very well with the naive perturbative estimate. In the future, one could try to compute both *T* and *P* hadronic matrix elements entirely with the LCSRs method. In that case, one would be able to predict the relative strong phases and thereby arrive at a more robust SM prediction for ΔA_{CP}. Further general arguments in favor of a small SM expectation for direct *CP* violation in the charm sector may be found in Reference 113.

In contrast, the authors of Reference 109 assert that the magnitude of ΔA_{CP} is consistent with having an SM origin. They employ *U* spin and SU(3) flavor symmetry and conclude that only modest $SU(3)_F$ breaking is required to generate the observed value. This breaking can come through either perturbative effects or nonperturbative enhancement due to rescattering. Similar conclusions are reached in Reference 114.

Thus, we are in the unfortunate situation that perturbative and sum-rule estimates are at least one order of magnitude below the experimental value, while symmetry-based approaches suggest that the SM is in perfect agreement with data. To identify the true origin of direct *CP* violation in the charm sector, greater theoretical understanding is necessary. Furthermore, new measurements in control channels (see Section 5.3.3) will be invaluable in confronting the SM predictions arising from the above approaches.

5.3.2. BSM explanations. The possibility that the value of ΔA_{CP} is driven by BSM effects was recently investigated in References 93, 112, and 115. Chala et al. (112) proposed a Z' model that is severely constrained by *D* mixing, but not yet ruled out. Dery & Nir (115) studied ΔA_{CP} in the context of the two-Higgs-doublet model, minimal supersymmetry, and models with vector-like up quarks, also taking into account ϵ'/ϵ bounds from the kaon sector. Hiller and colleagues (93) considered more general Z' models to explain ΔA_{CP} and also assessed their consequences for rare charm decays. In that study, the severe constraints from *D* mixing were considerably softened by allowing BSM contributions with different chiralities, which can cancel in the mixing.

5.3.3. Control measurements. Further experimental studies are desirable to elucidate the currently unclear theory situation, and several decay channels are proposed for investigation.

To validate the symmetry-based approaches, several measurements are desirable. For instance, it is noted that U spin predicts the important relation $a_{\rm dir}(K^+K^-) = -a_{\rm dir}(\pi^+\pi^-)$ (see, e.g., Reference 106), which strongly motivates individual determinations of the two asymmetries. Taking first-order $SU(3)_F$ corrections into account, one can derive a sum rule relating $a_{\rm dir}(K^+K^-)$ and $a_{\rm dir}(\pi^+\pi^-)$ with $a_{\rm dir}(\pi^0\pi^0)$, the corresponding *CP* asymmetry in $D^0 \to \pi^0\pi^0$ (116). In Reference 114, a long list of predictions for *CP* asymmetries is given based on symmetry considerations; promising modes include $D^0 \to \pi^+\rho^-$, $D^0 \to K^+K^{*-}$, $D^+ \to K^+K^{*0}$, $D^+ \to \eta\rho^+$, $D_s^+ \to \pi^+K^{*0}$, and $D_s^+ \to \pi^0K^{*+}$.

Another interesting option for control measurements is null tests—that is, decays that are expected to have a vanishing *CP* asymmetry in the SM. An example is the SCS mode $D^+ \to \pi^+\pi^0$, which has the same leading tree diagram as $D^0 \to \pi^+\pi^-$ but receives no contributions from a gluonic penguin amplitude because the final state has an isospin value of two. Thus, the SM expectation for the *CP* asymmetry of this decay is zero (117). Null tests involving rare charm decays are discussed in Reference 118.

Large *CP*-violating effects of up to 1% are expected in $D^0 \to K_S^0K_S^0$ within the SM, as explained in, for instance, Reference 119. Similarly, the *CP* asymmetry in $D^0 \to K^{*0}K_S^0$ can be as large as 0.3% (120). Additional examples of control channels can be found in Reference 108.

5.4. Analysis of Multibody Decays

Any direct *CP* violation present in a multibody decay will vary over phase space and has the possibility of being larger than in the two-body case because of interference effects between resonances. For these systems, therefore, *CP*-violation studies must be optimized to search for phase space–dependent differences in behavior between the charm and anticharm decays. This change in strategy brings some experimental benefits. For example, tagging and production asymmetries are no longer a primary concern, as they can induce a global offset only in measured rates, although correlations with the trigger and reconstruction of the signal decay may lead to this offset acquiring some nonuniformity at second order.

The LHCb Collaboration has analyzed data sets of 1.0 to 3.0 fb^{-1} to study the modes $D^+ \to \pi^+\pi^-\pi^+$ (121), $D^0 \to \pi^+\pi^-\pi^0$ (16), $D^0 \to K_S^0K^\mp\pi^\pm$ (122), $D^0 \to \pi^+\pi^-\pi^+\pi^-$ (123, 124), and $D^0 \to K^+K^-\pi^+\pi^-$ (124–126). The *B* factories performed important studies of the channels $D^+ \to K^+K^-\pi^+$ (127), $D^0 \to \pi^+\pi^-\pi^0$ and $K^+K^-\pi^0$ (128), $D^+ \to K^+K_S^0\pi^+\pi^-$ (129), and $D^0 \to K^+K^-\pi^+\pi^-$ (130, 131). All results are consistent with *CP* conservation. No analysis of interesting sensitivity has yet been made of multibody D_s^+ meson decays. The LHCb Run 2 sample remains to be exploited for multibody measurements and has the potential to bring a great improvement in precision.

CP-violation searches in phase space can be performed in either a model-dependent or model-independent manner. In the former, an amplitude model is constructed and then fitted separately to the charm and anticharm decay samples (122, 125, 127, 128). Significant differences in the amplitude modulus, phase, or fit fraction of any resonance contribution between the two data sets would signify the presence of *CP* violation. This approach has the virtue of targeting those regions of phase space where intermediate states are known to exist, and yielding results that are straightforward to interpret. For example, in the $D^0 \to K^+K^-\pi^+\pi^-$ study of LHCb, *CP* asymmetries related to the amplitude modulus, phase, and fit fraction were determined with uncertainties of 1% to 15%, depending on the resonance (125).

A simple model-independent procedure is to partition phase space into bins and then search for significant differences in the bin contents between charm and anticharm decays (121, 124, 127, 128, 132) (see, e.g., **Figure 6**). Unbinned approaches include the study of angular moments of the

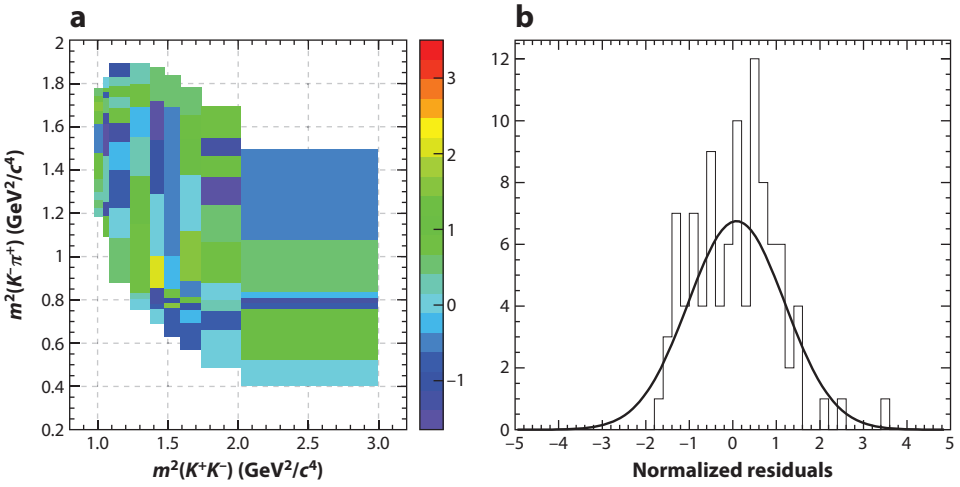

Figure 6

(*a*) Search for local *CP* violation in $D^+ \to K^+K^-\pi^+$ decays. (*b*) Normalized residuals, expressing the difference between D^+ and D^- decays, are determined in suitably chosen bins of the Dalitz plot. Adapted with permission from Reference 127.

intensity distributions (127, 128), the *k*-nearest neighbor method (121, 133–135), and the so-called energy test (16, 123, 136). When the energy test is applied to the channel $D^0 \to \pi^+\pi^-\pi^+\pi^-$ in the LHCb Run 1 data sample, the *P*-odd *CP* asymmetries are found to be only marginally consistent with the *CP*-conservation hypothesis (123), making this mode of particular interest for future analyses.

An alternative class of model-independent analysis involves triple-product asymmetries, such as *T*-odd moments, which probe *CP* violation through differential distributions (137, 138). This strategy, which can be regarded as complementary to those based on studies of *CP* asymmetries, has been employed at LHCb and the *B* factories to study the decays $D^0 \to K^+K^-\pi^+\pi^-$ (126, 130, 131) and $D^+ \to K^+K^0_S\pi^+\pi^-$ (129).

5.5. Searches for *CP* Violation in Charm Baryon Decays

CP violation in baryon decays remains a largely unexplored domain. Systematic control is challenging because most measurements require understanding the different interaction cross sections of protons and antiprotons. The LHCb Collaboration performed a study analogous to the two-body ΔA_{CP} measurement to determine the difference in phase space–integrated *CP* asymmetries between the modes $\Lambda_c^+ \to pK^+K^-$ and $\Lambda_c^+ \to p\pi^+\pi^-$ and achieved a precision of 1% with Run 1 data (139). The LHCb Collaboration also has searched for local *CP* asymmetries within the phase space of the decay $\Xi_c^+ \to pK^-\pi^+$ (140). In baryon decays, it is possible to probe for *CP* violation by measuring the weak asymmetry parameter α in an angular analysis (141) and comparing the results for charm and anticharm decays. Until now, this method has been deployed only in CF decays (142, 143).

6. CONCLUSIONS AND OUTLOOK

The current era is the most exciting one in charm physics for many decades. Neutral mixing and *CP* violation, long feared to be too small for experimental study, are now observed, and the next

goals are firmly in sight. The most urgent tasks are to establish whether the parameter x, and hence the mass splitting in the neutral charm system, is of a similar magnitude to y, or instead vanishing; to make further measurements of direct CP violation, in particular those that will help elucidate whether the size of ΔA_{CP} is compatible with SM expectations; and finally to intensify the search for CP violation associated with $D^0\bar{D}^0$ oscillations. Fortunately, the prospects for meeting these challenges are excellent. Many key measurements are still to be performed on the Run 1 and Run 2 LHCb data sets, and soon complementary charm studies will emerge from Belle II. Even more excitingly, the vast increase in sample sizes that will become available at LHCb Upgrades I and II will allow for a corresponding advance in precision, as long as systematic control can be maintained. With this likely progress in mind, it is imperative that theoretical developments keep track. Here, considerable improvements in methods based on symmetry principles, HQE, LCSRs, and lattice QCD are foreseen.

Charm is now a fast-moving discipline—one that can be considered complementary to beauty for its potential to test the CKM paradigm and to probe for New Physics effects. For flavor physicists, this is truly the age of charm.

DISCLOSURE STATEMENT

The authors are not aware of any affiliations, memberships, funding, or financial holdings that might be perceived as affecting the objectivity of this review.

ACKNOWLEDGMENTS

A.L. would like to thank Maria Laura Piscopo, Aleksey Rusov, and Christos Vlahos for proofreading, checking some formulae, and creating **Figure 1**, and Marco Gersabeck and Alex Kagan for helpful discussions. G.W. would like to acknowledge the valuable input of Sneha Malde and Nathan Jurik.

LITERATURE CITED

1. Glashow SL, Iliopoulos J, Maiani L. *Phys. Rev. D* 2:1285 (1970)
2. Aubert JJ, et al. *Phys. Rev. Lett.* 33:1404 (1974)
3. Augustin JE, et al. *Phys. Rev. Lett.* 33:1406 (1974)
4. Buras A. *Gauge Theories of Weak Decays*. Cambridge, UK: Cambridge Univ. Press (2020)
5. Cabibbo N. *Phys. Rev. Lett.* 10:531 (1963)
6. Kobayashi M, Maskawa T. *Prog. Theor. Phys.* 49:652 (1973)
7. Buchalla G, Buras AJ, Lautenbacher ME. *Rev. Mod. Phys.* 68:1125 (1996)
8. Charles J, et al. *Eur. Phys. J. C* 41:1 (2005)
9. Bona M, et al. *J. High Energy Phys.* 0610:081 (2006)
10. Ko B, et al. *Phys. Rev. Lett.* 112:111801 (2014). Erratum. *Phys. Rev. Lett.* 112:139903 (2014)
11. Lees J, et al. *Phys. Rev. D* 93:112014 (2016)
12. Peng T, et al. *Phys. Rev. D* 89:091103 (2014)
13. Aaltonen TA, et al. *Phys. Rev. Lett.* 111:231802 (2013)
14. Aaltonen T, et al. *Phys. Rev. D* 86:032007 (2012)
15. Aaij R, et al. *Phys. Rev. D* 97:031101 (2018)
16. Aaij R, et al. *Phys. Lett. B* 740:158 (2015)
17. Aaij R, et al. *Phys. Rev. Lett.* 122:231802 (2019)
18. Kou E, et al. *Prog. Theor. Exp. Phys.* 2019:123C01 (2019)
19. Bediaga I, et al. arXiv:1808.08865 [hep-ex] (2018)
20. Aaij R, et al. *J. High Energy Phys.* 1603:159 (2016). Erratum. *J. High Energy Phys.* 1609:13 (2016). Erratum. *J. High Energy Phys.* 1705:74 (2017)

21. Ablikim M, et al. *Chin. Phys. C* 44:040001 (2020)
22. Ablikim M, et al. *Phys. Rev. D* 101:112002 (2020)
23. Luo Q, et al. Progress of conceptual study for the accelerators of a 2-7GeV super tau charm facility at China. In *Proceedings of the 10th International Particle Accelerator Conference*, ed. M Boland, H Tanaka, D Button, R Dowd, VRW Schaa, E Tan, pp. 643–45. Geneva: JACoW Publ. (2019)
24. Eidelman S. *Nucl. Part. Phys. Proc.* 260:238 (2015)
25. Abada A, et al. *Eur. Phys. J. C* 79:474 (2019)
26. Ahdida CC, et al. *SPS Beam Dump Facility comprehensive design study*. Tech. Rep. CERN-PBC-REPORT-2018-001, CERN, Geneva (2018)
27. Ellis RK, et al. (Eur. Strategy Part. Phys. Prep. Group) arXiv:1910.11775 [hep-ex] (2019)
28. Nierste U. arXiv:0904.1869 [hep-ph] (2009)
29. Jubb T, Kirk M, Lenz A, Tetlalmatzi-Xolocotzi G. *Nucl. Phys. B* 915:431 (2017)
30. Kagan AL, Sokoloff MD. *Phys. Rev. D* 80:076008 (2009)
31. Kagan AL, Silvestrini L. arXiv:2001.07207 [hep-ph] (2020)
32. Bergmann S, et al. *Phys. Lett. B* 486:418 (2000)
33. Nir Y. *CP* violation in meson decays. In *Particle Physics Beyond the Standard Model*, Vol. 84: *Lecture Notes of the Les Houches Summer School 2005*, ed. D Kazakov, S Lavignac, J Dalibard, pp. 79–145. Amsterdam, Netherlands: Elsevier (2006)
34. Khoze VA, Shifman MA. *Sov. Phys. Usp.* 26:387 (1983)
35. Shifman MA, Voloshin M. *Sov. J. Nucl. Phys.* 41:120 (1985)
36. Bigi II, Uraltsev N. *Phys. Lett. B* 280:271 (1992)
37. Bigi II, Uraltsev N, Vainshtein A. *Phys. Lett. B* 293:430 (1992). Erratum. *Phys. Lett. B* 297:477 (1992)
38. Blok B, Shifman MA. *Nucl. Phys. B* 399:441 (1993)
39. Blok B, Shifman MA. *Nucl. Phys. B* 399:459 (1993)
40. Beneke M, et al. *Phys. Lett. B* 459:631 (1999)
41. Lenz A. *Int. J. Mod. Phys. A* 30:1543005 (2015)
42. Artuso M, Borissov G, Lenz A. *Rev. Mod. Phys.* 88:045002 (2016). Erratum. *Rev. Mod. Phys.* 91:049901 (2019)
43. Kirk M, Lenz A, Rauh T. *J. High Energy Phys.* 1712:68 (2017). Erratum. *J. High Energy Phys.* 2006:162 (2020)
44. Lenz A, Rauh T. *Phys. Rev. D* 88:034004 (2013)
45. Carrasco N, et al. *Phys. Rev. D* 90:014502 (2014)
46. Carrasco N, et al. *Phys. Rev. D* 92:034516 (2015)
47. Bazavov A, et al. *Phys. Rev. D* 97:034513 (2018)
48. Lenz A. *Proc. Sci.* CHARM2016:003 (2017)
49. Lenz A, Piscopo ML, Vlahos C. *Phys. Rev. D* 102:093002 (2020)
50. Georgi H. *Phys. Lett. B* 297:353 (1992)
51. Ohl T, Ricciardi G, Simmons EH. *Nucl. Phys. B* 403:605 (1993)
52. Bigi II, Uraltsev NG. *Nucl. Phys. B* 592:92 (2001)
53. Bobrowski M, Lenz A, Riedl J, Rohrwild J. *J. High Energy Phys.* 1003:9 (2010)
54. Bobrowski M, Lenz A, Rauh T. arXiv:1208.6438 [hep-ph] (2012)
55. Asatrian H, Hovhannisyan A, Nierste U, Yeghiazaryan A. *J. High Energy Phys.* 1710:191 (2017)
56. Asatrian HM, et al. *Phys. Rev. D* 102:033007 (2020)
57. Wolfenstein L. *Phys. Lett. B* 164:170 (1985)
58. Donoghue JF, Golowich E, Holstein BR, Trampetic J. *Phys. Rev. D* 33:179 (1986)
59. Falk AF, Grossman Y, Ligeti Z, Petrov AA. *Phys. Rev. D* 65:054034 (2002)
60. Cheng HY, Chiang CW. *Phys. Rev. D* 81:114020 (2010)
61. Jiang HY, et al. *Chin. Phys. C* 42:063101 (2018)
62. Hansen MT, Sharpe SR. *Phys. Rev. D* 86:016007 (2012)
63. Falk AF, et al. *Phys. Rev. D* 69:114021 (2004)
64. Li HN, Umeeda H, Xu F, Yu FS. *Phys. Lett. B* 810:135802 (2020)
65. Amhis YS, et al. arXiv:1909.12524 [hep-ex] (2019)

66. Aaij R, et al. *Phys. Rev. Lett.* 110:101802 (2013)
67. Aaij R, et al. *Phys. Rev. Lett.* 122:011802 (2019)
68. Zupanc A, et al. *Phys. Rev. D* 80:052006 (2009)
69. Starič M, et al. *Phys. Lett. B* 753:412 (2016)
70. Aaltonen TA, et al. *Phys. Rev. D* 90:111103 (2014)
71. Lees J, et al. *Phys. Rev. D* 87:012004 (2013)
72. Aaij R, et al. *Phys. Rev. Lett.* 118:261803 (2017)
73. Aaij R, et al. *Phys. Rev. D* 101:012005 (2020)
74. Nayak M, et al. *Phys. Rev. D* 102:071102(R) (2020)
75. Malde S, Thomas C, Wilkinson G. *Phys. Rev. D* 91:094032 (2015)
76. Harnew S, Rademacker J. *Phys. Lett. B* 728:296 (2014)
77. Atwood D, Soni A. *Phys. Rev. D* 68:033003 (2003)
78. Lowrey N, et al. *Phys. Rev. D* 80:031105 (2009)
79. Evans T, et al. *Phys. Lett. B* 757:520 (2016). Erratum. *Phys. Lett. B* 765:402 (2017)
80. Aaij R, et al. *Phys. Rev. Lett.* 116:241801 (2016)
81. Evans T, Libby J, Malde S, Wilkinson G. *Phys. Lett. B* 802:135188 (2020)
82. Aubert B, et al. *Phys. Rev. Lett.* 103:211801 (2009)
83. Asner D, et al. *Phys. Rev. D* 72:012001 (2005)
84. Libby J, et al. *Phys. Rev. D* 82:112006 (2010)
85. Bondar A, Poluektov A, Vorobiev V. *Phys. Rev. D* 82:034033 (2010)
86. Thomas C, Wilkinson G. *J. High Energy Phys.* 1210:185 (2012)
87. Di Canto A, et al. *Phys. Rev. D* 99:012007 (2019)
88. del Amo Sanchez P, et al. *Phys. Rev. Lett.* 105:081803 (2010)
89. Abe K, et al. *Phys. Rev. Lett.* 99:131803 (2007)
90. Golowich E, Hewett J, Pakvasa S, Petrov AA. *Phys. Rev. D* 76:095009 (2007)
91. Silvestrini L. arXiv:1510.05797 [hep-ph] (2015)
92. Bona M, et al. *J. High Energy Phys.* 0803:049 (2008)
93. Bause R, Gisbert H, Golz M, Hiller G. *Phys. Rev. D* 101:115006 (2020)
94. Fajfer S, Košnik N. *Phys. Rev. D* 87:054026 (2013)
95. Aaij R, et al. *Phys. Lett. B* 767:177 (2017)
96. Aaltonen T, et al. *Phys. Rev. D* 85:012009 (2012)
97. Nisar N, et al. *Phys. Rev. Lett.* 112:211601 (2014)
98. Dash N, et al. *Phys. Rev. Lett.* 119:171801 (2017)
99. Babu V, et al. *Phys. Rev. D* 97:011101 (2018)
100. Aaij R, et al. *Phys. Rev. Lett.* 122:191803 (2019)
101. Mendez H, et al. *Phys. Rev. D* 81:052013 (2010)
102. Aaij R, et al. *Phys. Rev. Lett.* 122:211803 (2019)
103. Aaij R, et al. *J. High Energy Phys.* 1407:41 (2014)
104. Aaij R, et al. *Phys. Rev. Lett.* 116:191601 (2016)
105. Zyla P, et al. *PTEP* 2020:083C01 (2020)
106. Grossman Y, Kagan AL, Nir Y. *Phys. Rev. D* 75:036008 (2007)
107. Bigi II, Paul A, Recksiegel S. *J. High Energy Phys.* 1106:89 (2011)
108. Lenz A. arXiv:1311.6447 [hep-ph] (2013)
109. Grossman Y, Schacht S. *J. High Energy Phys.* 1907:20 (2019)
110. Balitsky I, Braun VM, Kolesnichenko A. *Nucl. Phys. B* 312:509 (1989)
111. Khodjamirian A, Petrov AA. *Phys. Lett. B* 774:235 (2017)
112. Chala M, Lenz A, Rusov AV, Scholtz J. *J. High Energy Phys.* 1907:161 (2019)
113. Nierste U. *Proc. Sci.* Beauty2019:048 (2020)
114. Cheng HY, Chiang CW. *Phys. Rev. D* 100:093002 (2019)
115. Dery A, Nir Y. *J. High Energy Phys.* 1912:104 (2019)
116. Müller S, Nierste U, Schacht S. *Phys. Rev. Lett.* 115:251802 (2015)
117. Brod J, Kagan AL, Zupan J. *Phys. Rev. D* 86:014023 (2012)

118. Bause R, Golz M, Hiller G, Tayduganov A. *Eur. Phys. J. C* 80:65 (2020)
119. Nierste U, Schacht S. *Phys. Rev. D* 92:054036 (2015)
120. Nierste U, Schacht S. *Phys. Rev. Lett.* 119:251801 (2017)
121. Aaij R, et al. *Phys. Lett. B* 728:585 (2014)
122. Aaij R, et al. *Phys. Rev. D* 93:052018 (2016)
123. Aaij R, et al. *Phys. Lett. B* 769:345 (2017)
124. Aaij R, et al. *Phys. Lett. B* 726:623 (2013)
125. Aaij R, et al. *J. High Energy Phys.* 1902:126 (2019)
126. Aaij R, et al. *J. High Energy Phys.* 1410:5 (2014)
127. Lees J, et al. *Phys. Rev. D* 87:052010 (2013)
128. Aubert B, et al. *Phys. Rev. D* 78:051102 (2008)
129. Lees J, et al. *Phys. Rev. D* 84:031103 (2011)
130. del Amo Sanchez P, et al. *Phys. Rev. D* 81:111103 (2010)
131. Kim J, et al. *Phys. Rev. D* 99:011104 (2019)
132. Bediaga I, et al. *Phys. Rev. D* 80:096006 (2009)
133. Williams M. *J. Instrum.* 5:P09004 (2010)
134. Henze N. *Ann. Stat.* 16:772 (1988)
135. Schilling MF. *J. Am. Stat. Assoc.* 81:799 (1986)
136. Williams M. *Phys. Rev. D* 84:054015 (2011)
137. Bigi II. arXiv:hep-ph/0107102 (2001)
138. Durieux G, Grossman Y. *Phys. Rev. D* 92:076013 (2015)
139. Aaij R, et al. *J. High Energy Phys.* 1803:182 (2018)
140. Aaij R, et al. *Eur. Phys. J. C* 80:986 (2020)
141. Korner J, Kramer M. *Phys. Lett. B* 275:495 (1992)
142. Hinson J, et al. *Phys. Rev. Lett.* 94:191801 (2005)
143. Link J, et al. *Phys. Lett. B* 634:165 (2006)

Annual Review of Nuclear and Particle Science

Volume 71, 2021

Contents

Errata

An online log of corrections to *Annual Review of Nuclear and Particle Science* articles may be found at http://www.annualreviews.org/errata/nucl